1 INTRODUCTION

South Africa has an established hardmetal cutting tool industry. Nevertheless, the coated cutting tool market is shared by imported products and locally produced products. The customers, who have access to all these products, have experienced differences in the products' performance. It has been noticed that products from different suppliers exhibit different performances although when aimed at the same application. Therefore, a need was felt to determine why some coated cutting tool inserts perform better than others. Thus, cutting tool inserts from five of the best suppliers were investigated to determine the reasons for their different performance.

The properties of coated hardmetal cutting tool inserts vary with their application. This investigation focused on cutting tool inserts of the main machining group P (according to ISO 513 [Brookes, 1998]). The hardmetal grades of this group contain, besides WC, TiC, TaC and/or NbC in the form of mixed crystals with WC. They are distinguished by their excellent high-temperature strength and low abrasion and are used for the turning of steel (ferrous metal) which generates long chips.

Nowadays, different coating technologies are in practice to coat tool inserts. The production of multilayer coatings which combine useful properties of different materials is now standard. All tool inserts investigated in the present research project were coated by Chemical Vapor Deposition (CVD).

The requirements of a good cutting tool insert for turning are high hardness and high fracture toughness, as well as high wear resistance and good adhesion of the substrate to the coating. Therefore theses are the properties that were assessed in this investigation. Unfortunately, high temperature tests could not be included, for lack of suitable equipment.

The five types of inserts were compared by analyzing the substrate, the coating system and the interface between substrate and coating.

This involved mainly the analysis of the composition and microstructure of the substrates as well as of the various coating layers. In all cases, the techniques used were Scanning Electron Microscopy (SEM), Electron Dispersive Energy (EDS) analysis, X-ray diffraction, microprobe analysis and image analysis for grain size measurements on the substrate.

Besides the microstructure and composition, the properties of the various cutting tool inserts were also compared. This involved hardness tests, which aimed not only at measuring the hardness of substrates and coatings but also at generating cracks and comparing crack patterns. Wear resistance was measured by developing a “pin-on-disk” system and examining the wear scars. For adhesion assessment, the tests carried out involved cracks nucleated by Rockwell hardness indentations, three-point-bending tests, and scratch tests.

The results of the tests allowed to rank the inserts from “best” to “worst” on the basis of the properties investigated and conclusions were drawn on the properties that most affect the performance. The results of microstructure and composition analyses allowed to suggest which are the microstructure and composition that yield best performance.

The thesis is divided into six chapters. The current chapter presents the motivation for the investigation. Chapter 2 summarizes research done by other investigators in the field of coated cutting tool inserts. The samples, the experimental procedures, the methodology and the equipment employed are described in Chapter 3. The next two chapters (4 and 5) present the results of the analyses and experiments done, on the cutting tool substrates and on the coatings, respectively. Chapter 6 includes a general discussion of the results, conclusions and suggestions for further work. The thesis ends with a list of the references used and the appendices, where Appendix F contains reprints of papers published before submission of the thesis.

2 LITERATURE SURVEY

The current chapter contains background information on coated cutting tool inserts used in turning. It starts with describing cutting tool inserts and the application of turning. Then, substrates based on WC-Co are introduced, as well as the coating technique of CVD (Chemical Vapor Deposition). The coatings encountered in this research project are described, i.e. TiC, TiN, TiCN and Al_2O_3. Results of mechanical properties of cemented carbides and coated cemented carbides, such as hardness, wear resistance and adhesion are reported.

2.1 Hardmetal Cutting Tools Used in Turning

In our everyday life many tools and equipments we use are machined from steel. To get the required shapes and forms, a cutting tool material is needed which is harder than steel, such as hardmetals. The most important properties for cutting tool inserts are low friction coefficient, oxidation resistance, chemical stability, hot hardness, abrasive wear resistance, crack resistance and good thermal properties [Kalss, 2005].

The present project deals with hardmetal cutting tool inserts consisting of a substrate and a coating. The substrate is based on WC-Co, which is milled, pressed and then sintered at about 1350 to 1450 °C. A cutting tool with its main components is displayed in Fig. 2.1 [Boothroyed, 1981].

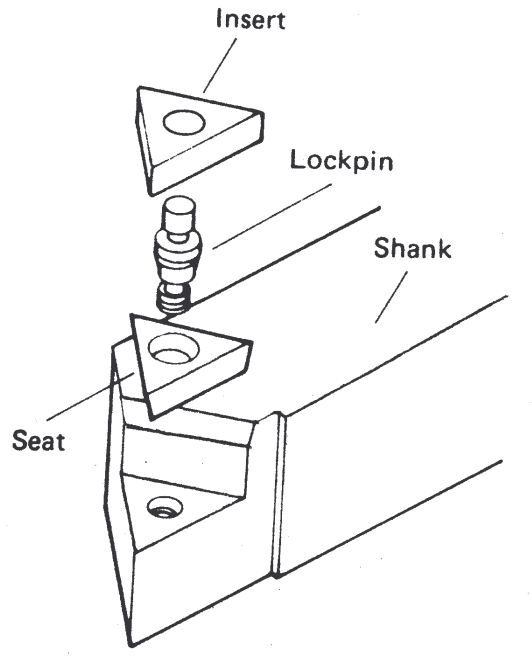

Fig. 2.1: Typical style of clamped-on (throw-away) insert tool [Boothroyed, 1981]

Cutting tool inserts cut metal because they are sharp and harder than the workpiece. The insert is attached with the lockpin to the seat and then it is fixed with the same pin to the shank or holder. When all cutting edges have been worn, the insert is thrown away.

The cutting tool inserts investigated in the present project are all used for turning. This operation generates cylindrical shapes with a single point tool where the tool is stationary and the workpiece rotates (see Fig. 2.2 [AB Sandvik, 1994]).

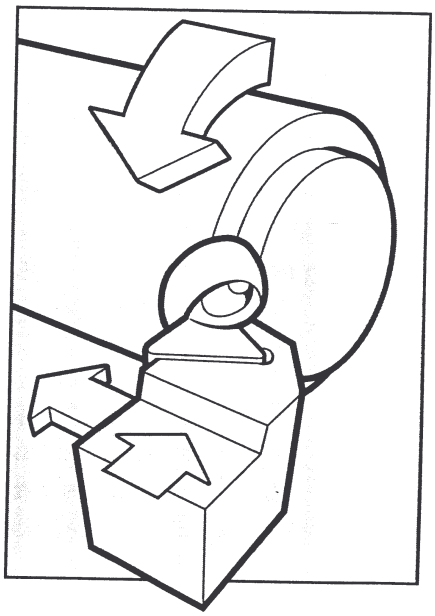

Fig. 2.2: Cutting tool insert for turning processes [AB Sandvik, 1994]

Turning involves two movements, the rotation of the workpiece and the feed of the tool. The cutting speed or surface speed in m/min is given by:

$$v_c = \frac{D \cdot \pi \cdot n}{1000} \qquad \text{(m/min)}$$

where: D: diameter of the workpiece in mm
n: rotational velocity in rpm

as indicated in Fig. 2.3 [AB Sandvik, 1994].

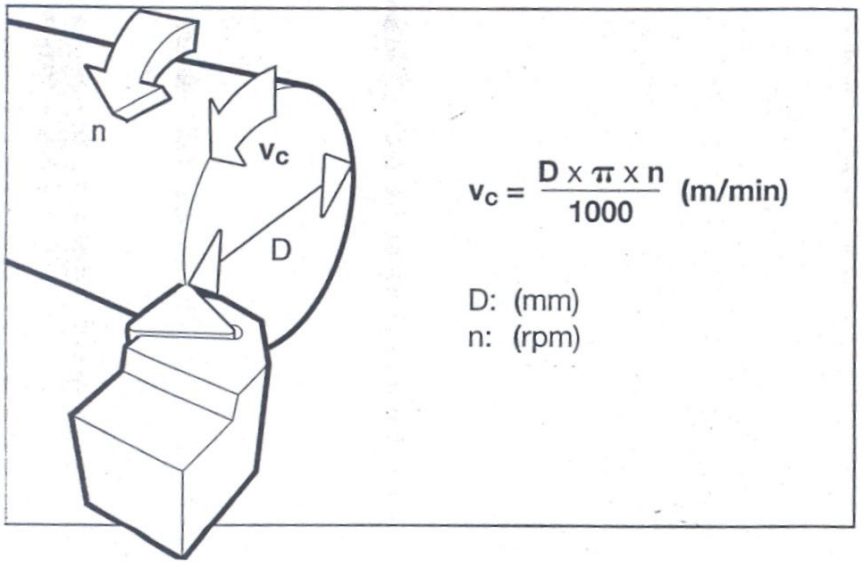

Fig. 2.3: Definition of cutting speed (v_c) [AB Sandvik, 1994]

In Fig. 2.2, the metal turning process has already started, as a formed chip can be identified. In metal cutting, the cut material generates chips which flow over the rake face of the tool and which shape and size depend on the geometry of the cutting insert. A sketch of chip formation and relevant definitions can be seen in Fig. 2.4 [König-b].

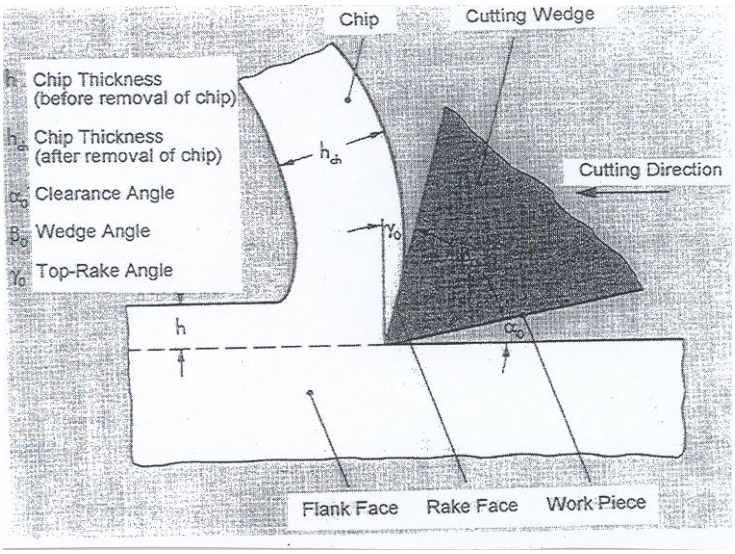

Fig. 2.4: Chip formation [König-b]

The chips remove metal during the cutting process, and also remove generated heat. When designing an insert, the temperature control, the forces and the chip formation during the cutting process have to be taken into consideration. Different shapes of chips are shown in Fig. 2.5 [König-b].

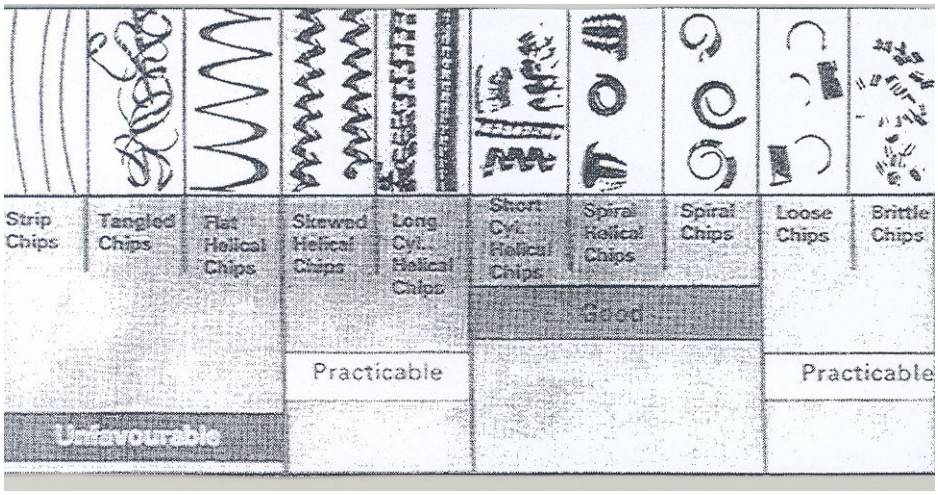

Fig. 2.5: Chip shapes produced during turning [König-b]

Strip chips, tangled chips and flat helical chips are unfavorable as they make removal of the chips difficult while short cylindrical helical chips, spiral helical chips and spiral chips are good removal mediums. The other four chip shapes in Fig. 2.5 are considered acceptable.

2.2 Cemented Carbide Substrates Based on WC-Co

The present project investigates coated cutting tool inserts, which consist of substrate and coating. The substrate consists of carbides cemented by a Co-rich binder phase. To improve the wear resistance of a pure WC-Co substrate, another phase is often added, the cubic transitional metal carbides (W,Ti,Ta,Nb)C. The main phase WC has a simple hexagonal crystal structures and two atoms per unit cell, with W atoms at (0,0,0) positions and C atoms at positions (2/3,1/3,1/2) [Exner, 1979].

The binder consists usually of Co with some C and W in solid solution. Its weight percent is much lower than that of WC (5 - 25 wt.%). Co appears in two modifications, hcp and fcc. In cemented carbides the Co is usually in the fcc form because C and W dissolved in it and residual stresses hinder the fcc → hcp transformation. Exner [Exner, 1979] states that the amount of W in solid solution is an inverse function of the C content of the binder. This means that an increase in the C content results in decreased dissolved W and vice versa. A section of the Co-W-C ternary phase diagram at 1273 K is shown in Fig. 2.6 [Vuorinen, 1993].

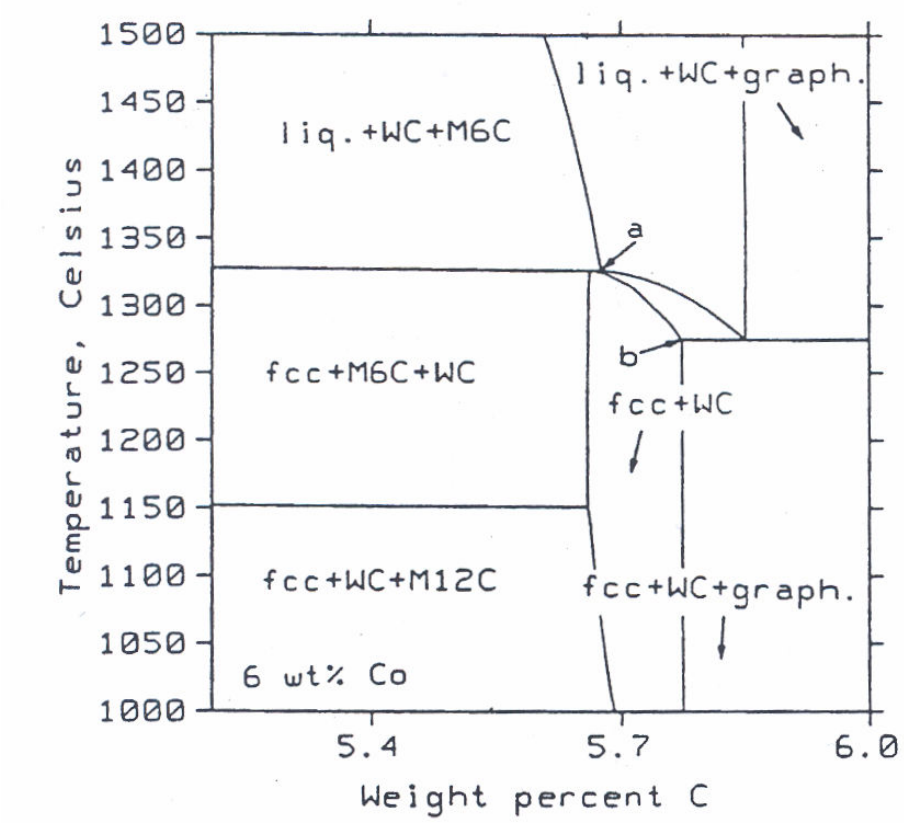

Fig. 2.6: Section of the Co-W-C ternary phase diagram at 1273 K for WC – 6 wt.% Co (M6C and M12C = eta-carbide, fcc = Co) [Vuorinen, 1993]

It can be seen that the two-phase region in WC-Co (or three-phase field in WC-Co-γ cemented carbides, where γ = mixed metal carbides) is very narrow with respect to the C content of the alloy and a very small change in the C content will bring the alloy into a three-phase field (or four-phase field in WC-Co-γ). Eta-carbide will form if there is not enough C present and any C excess will result in C porosity. As eta-carbides and porosity affect negatively the properties of a substrate, the C content during sintering has to be kept within the field marked between a and b in Fig. 2.6, where a corresponds to 5.68 wt.% C and b to 5.77 wt.% C. In a WC-Co substrate with 6 wt.% Co, the sintering process is controlled so that both (eta-carbides and porosity) are avoided.

Exner [Exner, 1983] described cemented carbides as single crystals of one or more carbide phases which form a continuous skeleton (at low Co contents) where the free space is filled by a metal binder. The microstructure of cemented carbide influences its properties, the most important features being the mean grain size of the carbide crystals, the mean free path in the binder phase and the contiguity of the carbide skeleton.
The binder phase fills the spaces within the carbide skeleton during the liquid phase sintering process and forms interfaces between the binder phase and the carbide phases and between the grain boundaries in the binder phase. Exner [Exner, 1983] reported that very coarse Co grains develop during cooling after the sintering process depending on the cooling rate, as shown in Fig. 2.7 [Exner, 1983].

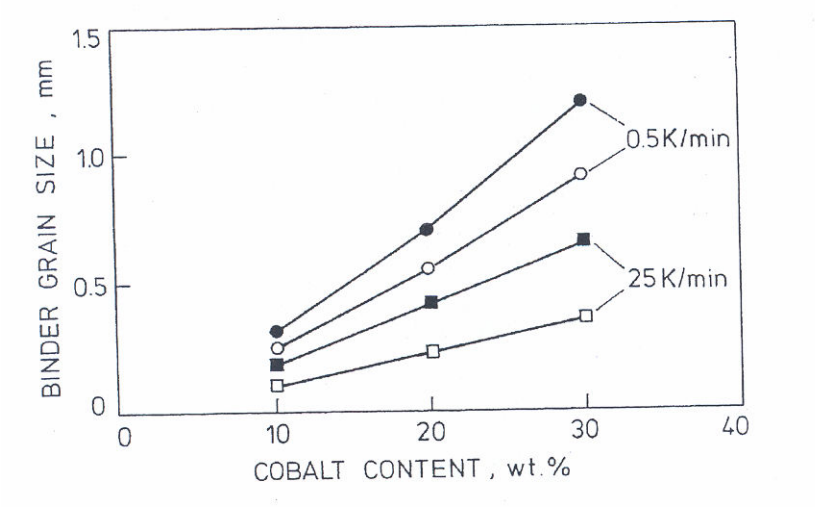

Fig. 2.7: The variation of the grain size with Co content, C content and cooling rate. The full symbols indicate a low, the open symbols a high C content of the alloys. [Exner, 1983]

Another important parameter which affects the mechanical behavior of the binder, is the mean free path. That parameter is the arithmetic mean of the distances from one carbide/binder interface to the other measured in the binder phase. In a single grain of the binder phase there are millions of carbide crystals. Therefore, the mean free path is two to four orders of magnitude smaller than the binder grain size.

As for the microstructure of the carbide phases, most impurities in the powders seem to have not an important effect on the carbide crystal growth in WC-Co [Exner, 1983]. WC has an anisotropic structure and therefore develops an anisotropic crystal shape which is described as "flat triangular prisms with truncated edges" [Exner, 1979]. WC exists only in a narrow range of C contents close to the stoichiometry of WC and it does not take other elements in solid solution. Mixed carbides powders, such as (W,Ti)C are not in equilibrium with the binder phase at sintering [Exner, 1979].

The geometry of the carbide skeleton affects the interactions between carbide and binder. This can be described by the contiguity, which is the ratio of grain boundary density to total surface density of the carbide crystals in the alloy. Nowadays, cemented carbides have low residual porosity. However, if found in this materials, these flaws may initiate fracture.

Due to different thermal expansion coefficients of WC and Co, thermal residual stresses are generated in the substrates when cooling down after sintering. Those residual stresses are compressive in WC and tensile in the Co [Coats, 2003].
The samples tested by Coats *et al.* [Coats, 2003] had different Co content (10, 20 and 40 wt.%) and different WC particle size (0.5, 1.0 and 3.0 and 5.0 μm). Stress was measured and correlated to WC particle size and Co content. It was found that the residual compressive stress in WC increases with increasing Co content and with decreasing grain size, as can be seen in Fig. 2.8 [Coats, 2003].

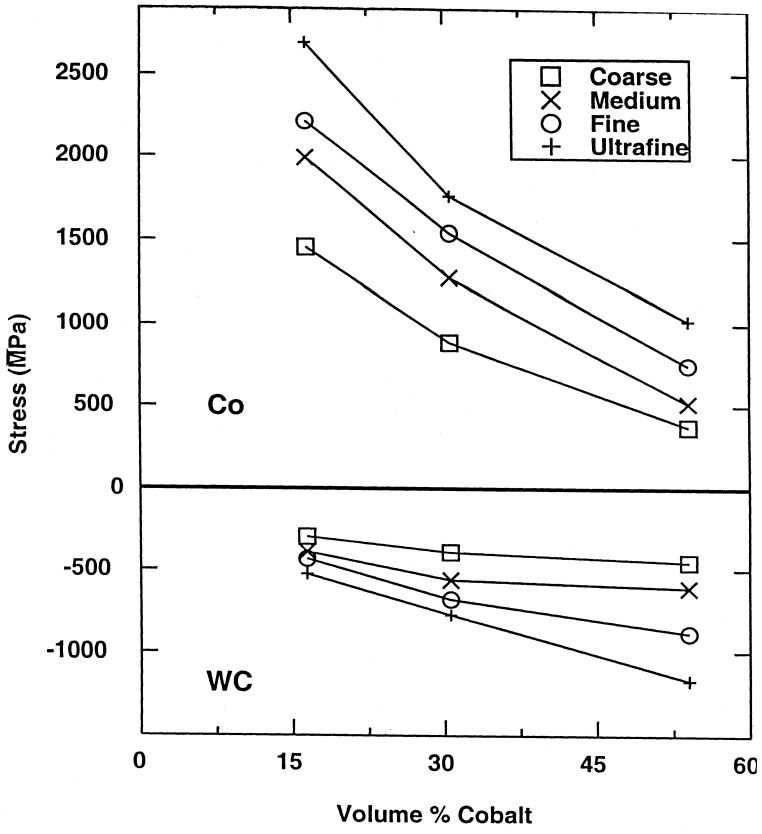

Fig 2.8: Residual stress in WC and Co vs. vol.% Co [Coats, 2003]

The graph in Fig. 2.8 shows stresses for WC-Co composites with varying WC particle size and Co-weight percentage. The stress in the Co is tensile, and the stress in the WC is compressive.

The tensile stress in the Co increases with decreasing Co content and decreasing WC particle size. The increasing stress with decreasing particle size can be explained by the reduction of the mean free path (MFP) of the Co. More constraint in the Co results and therefore the Co yield strength is increased.

With increasing thermal residual stresses, the stress distribution in the WC particles widens, as due to the angular WC particles the shear stress varies.

Carpenter [Carpenter, 1998] investigated parameters which influence the TRS of WC-Co hardmetals. The TRS can be used for quality control. Three-point-bending tests were done on cylindrical test samples with a loading rate of 1500 N/s. The stresses inside the cylinder are both in compression and tension, where tension tends to cause fracture more, especially close to the surface.

It was found that the TSR of fine hardmetals depends on the intrinsic strength of the microstructure, defects (> 20 μm) and the surface finish of the test pieces.

The surface preparation has a great influence on the strength of hardmetals, as residual stresses are introduced into the surface when grinding. To release residual compressive stresses induced by grinding, the samples can be annealed. Tests with untreated pieces and annealed pieces, showed that the fracture started from the interior of the untreated samples but for all annealed samples (at 1000 °C) fracture occurred at the surface [Carpenter, 1998].

The effects of C content were investigated, as they influence the mechanical properties. If there is high C content, graphite can be formed, whereas low C content can result in the unwanted brittle eta-phase.

The size of grains influence mechanical properties, usually the finer the sintered grains, the higher the hardness, and the lower the toughness and transverse rupture strength [Carpenter, 1998].

Impurity plays a further important role. There are always trace elements in hard metals, such as Ca, Al and Si. They can come from the raw material or external contamination. These elements can dissolve in the binder phase or even combine with O and S and precipitate. Carpenter [Carpenter, 1998] found when investigating the fracture surfaces that these impurities are often associated with pores. Failures from inclusions generally decrease the strength by an average of 20 – 30 %.

Schaller *et al.* [Schaller, 1992] investigated the mechanical behavior of WC with 11 wt.% Co by bending tests, internal friction and electron microscopy. During the cutting process, high temperatures develop which affect the behavior of hardmetals. Tests resulted in the definition of three temperature ranges according to their mechanical behavior. From room temperature up to 900 K, the material was elastic and brittle. Between 900 and 1100 K, a limited local plasticity was observed due to the strong hardening during deformation. Above 1100 K, the cemented carbide deformed and behaved according to creep curves.

Mechanical properties of WC-Co have been widely studied. Luyckx [Luyckx, 1984] found an empirical approach to the evaluation of the critical strain energy release rate (G_{IC}) in cemented carbides by means of Vickers indentations. O'Quigley *et al.* [O'Quigley, 1996] investigated the relationship between hardness and fracture toughness by testing WC-Co cemented carbides with different Co content (3 – 50 wt.%) and two mean grain sizes (2.2 and 6 μm). The following linear relationship was found:

$$H_v = -m\, K_{IC} + c$$

where: H_v: Vickers hardness
K_{IC}: fracture toughness
m, c: functions of WC grain size

At low toughness, grades of the same toughness showed a higher hardness with a fine mean grain size and vice versa at high toughness.

Extensive investigations into cemented carbides with the mixed carbides (W,Ti)C, which is one phase in the present project's substrates, have been done, e.g. by Doi *et al.* [Doi, 1984a].

One phenomenon which has been found when examining the cutting tool substrates was the use of so-called "graded substrates" by some of the cutting tool inserts (see section 4.2.4). A graded substrate consists of a surface zone with a rich binder phase and a depleted cubic phase. It is produced with a thin surface zone, approximately ± 20 μm wide which show a higher toughness compared to the bulk material.

The surface layer free of mixed carbides in the inserts' substrates has different properties than the bulk material. The reason for gradient substrates is to increase their toughness. A cemented carbide cutting tool based on WC-Co is often coated by CVD (Chemical Vapor Deposition) or PVD (Physical Vapor Deposition), see section 2.3, to increase its tool life. The coating process takes place at high temperatures, and during the cooling process cracks are often formed in the surface layers. Those cracks are of course undesirable as they can propagate during the cutting of the workpiece. To stop those cracks propagating, graded substrates are used with increased toughness which in turn increases the resistance to crack propagation. The present project deals with cemented carbides containing WC, the cubic phase (W,Ti)C and the binder Co. The hardest phase is the (W,Ti)C, however, it is also the most brittle phase. A cutting tool insert with a low (W,Ti)C fraction should have a higher toughness. However, decreasing the cubic phase would also reduce the hardness, which is undesirable. Therefore, a compromise is found by creating a tough surface layer in the substrate, and thus having the required hardness of the substrate and also a higher crack propagation resistance.

Schwarzkopf *et al*. [Schwarzkopf, 1988] studied the formation of surface zones free of cubic carbides. These zones could be achieved by outgassing N. The rate controlling step of that zone formation is the inward diffusion of metal atoms dissolved in the binder phase.

Cemented carbides with gradients created by outward N diffusion have usually three parts [Frykholm, 2001a] [Frykholm, 2001b]. The first part, close to the surface, is the layer depleted of cubic phase with an enriched binder phase. The second part is an area with a depletion of binder phase and enrichment of cubic phase. The third part is the bulk. The first two parts have different phase distribution. In the first part, the binder volume fraction increases from surface to zone border. Inside the zone border is a depletion of binder phase and an enrichment of cubic phase.

2.3 Coatings of Hardmetals by Chemical Vapor Deposition (CVD)

To improve tool life of cutting tool hardmetal inserts, the inserts were coated [Brookes, 1998]. That way, a higher toughness of the substrate with a higher wear resistance of the hard coating was achieved.

For turning applications, a coating thickness of ± 10 μm was chosen [Lux, 1987].

The history of cutting tool inserts starts around in the 1930s. Plain grades of WC and Co gave excellent results in cutting grey cast irons and hard non-ferrous metals, but they were not as useful in cutting steel because craters developed very rapidly, weakened the cutting edge and insert material just broke away (see Fig. 2.9).

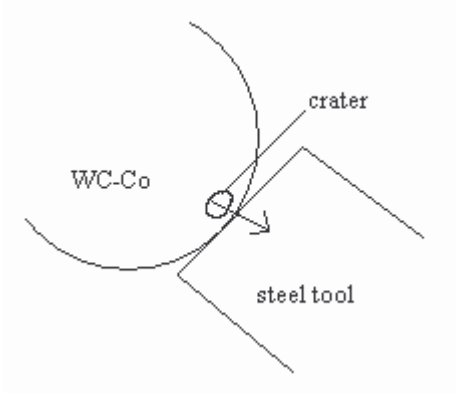

Fig. 2.9: Diffusion of W into Fe results in crater wear on chip face

Crater formation on the rake face is due to diffusion. The cutting tool material, in this case WC, dissolves in the workpiece, in this case steel. Solubility is temperature dependent and so the effect varies with the interface temperatures reached during metal cutting. During the cutting process, the temperatures can reach up to 900 °C.
When the cutting tool has a coating, this acts as a barrier to the diffusion of W into Fe.

Dearnley [Dearnley, 1985] reported wear investigations with coated and uncoated cemented carbides. It was found that the main reason for the success of coated inserts were the inherent resistance of the coated materials to dissolution or diffusion in the steel, which is the cause of rapid rake (crater) wear and relatively slower flank wear of the uncoated WC based cemented carbides at temperatures ~ 800 – 1200 °C [Dearnley, 1985].

The coating increases the wear resistance [Lux, 1989], also because the friction coefficient between the coating and the steel is lower than that between WC-Co and steel. That decrease in friction coefficient and in turn decreased heat development, results in a temperature reduction of the cutting wedge, and less diffusion between workpiece and cutting tool.

The coating materials are usually covalent/metallic bonded hard compounds such as carbides and nitrides (TiC, TiN, TiCN) and oxides (Al_2O_3). Nowadays,

multilayer coatings are deposited which are applied consecutively with improvements in properties as the individual grains of each layer are refined repeatedly due to nucleation of the phases.

The CVD process is complex ([Sundgren, 1986], [Pierson, 1992]). CVD is defined as the process of reacting gaseous constituents on a surface [Ettner, 1987]. With CVD it is possible to get coherent bonding of the coatings to the substrate. The hard materials for coatings used in the present project are listed in Table 2.1.

Table 2.1: Hard materials for the coating of tools tested in this project

Hard material	**Hardness value HV**	**Color**
TiC	3200	Grey-black
TiN	2100	Golden-yellow
TiCN	2500-3200	Yellow-brown to violet-black (depending on C:N)
Al_2O_3	2000	Grey to black

Generally, three steps are distinguished during a CVD reaction [Grainger, 1989]: firstly, a volatile carrier is produced; secondly, that gas is transported without decomposition to the deposition place and lastly, the chemical reactions take place and a coating is formed on the substrate, see Fig. 2.10 [Grainger, 1989]. The reactions are given in detail in section 2.4.

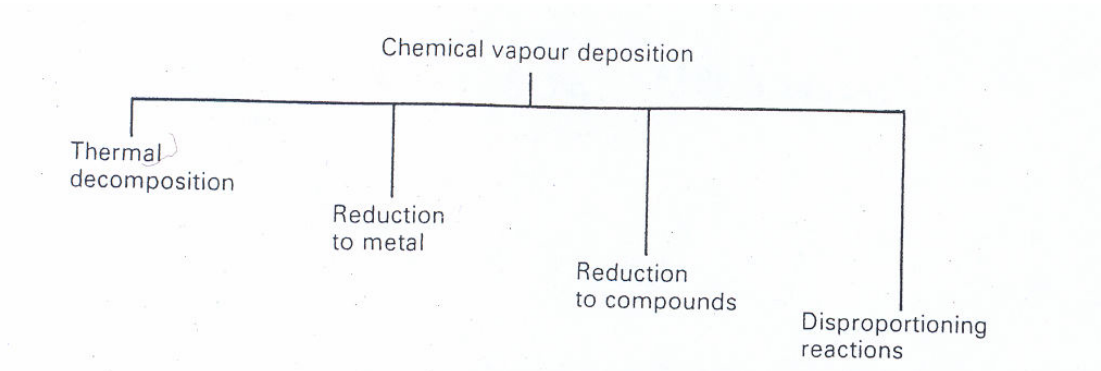

Fig. 2.10: Reactions involved in CVD [Grainger, 1989]

The most common CVD system is the closed reactor CVD. It consists of three components, the reactant supply, the deposition system or reactor and the exhaust system. The process sequence of a CVD coating plant is displayed schematically in Fig. 2.11 [Schedler, 1988].

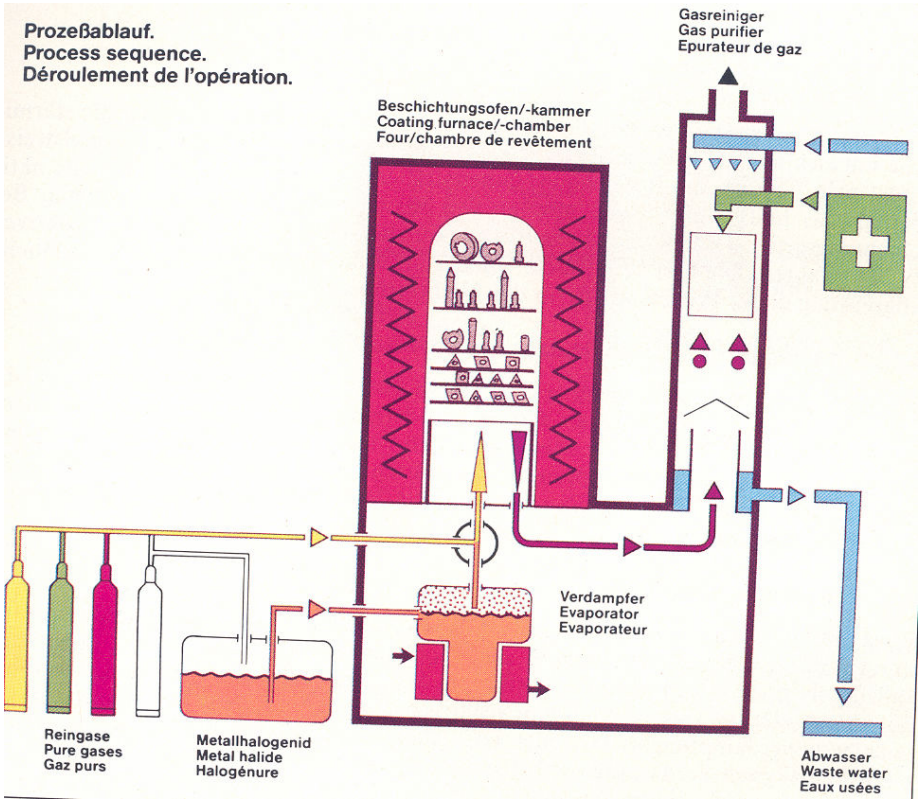

Fig. 2.11: Process sequence of a CVD coating plant [Schedler, 1988]

The whole process involves the following five steps:

1. Vaporization and transport of precursor molecules into reactor.
2. Diffusion of precursor molecules to surface.
3. Absorption of precursor molecules to surface.
4. Deposition of precursor and incorporation into solid films.
5. Recombination of molecular byproduct and desorbtion into gas phase.

One advantage of CVD is the range of materials that can be deposited. With CVD coatings good inherent properties (such as resistance to oxidation, high abrasive resistance, good adhesion to substrate, low thermal stress, etc.) are achieved, as

well as uniformity to provide consistent tool life, stable composition during cutting and economical production [Sivan, 1983].

When designing a coated cutting tool, four regions which determine coating characteristics must be considered [Carlsson, 1985] [Sarin, 1991] (see Fig. 2.12, [Sarin, 1991]).

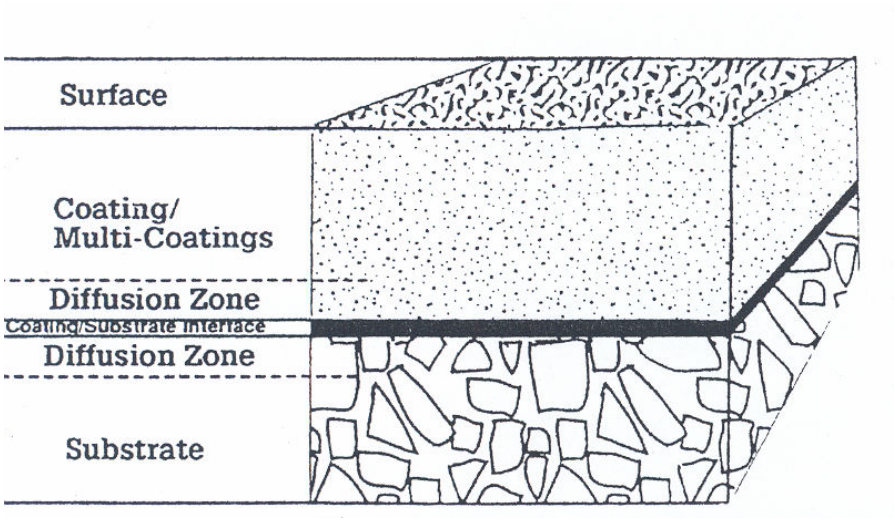

Fig. 2.12: The four critical regions in a CVD substrate/coating system that are critical to the design and development of any specific coating configuration [Sarin, 1991]

The substrate/coating interfacial region is vital. The strength of the bond at this interface has to be maximum to avoid interfacial failure. Adhesion is important, as at the substrate/coating interface, strains are generated due to different thermal expansion coefficients and different elastic properties between substrate and coating.

Most CVD films are deposited at high temperatures and at low deposition rates, which means that interdiffusion takes place, which usually results in good adhesion. The temperature during the coating process can be varied depending on the coating system. However, since thermodynamics and kinetics considerations take priority in the determination of the processing temperature for a coating

system, the flexibility in the choice of temperature is low. Low temperatures can also lead to undesirable diffusion, such as the formation of the eta-phase ($W_xCo_{12-x}C$) at the interface in the substrate due to C diffusion. As the eta-phase has a higher density that the substrate, unwanted porosity due to volume shrinkage results [Sarin, 1991].

The coating is designed according to the requirements. The coating compounds are selected by their chemical bonding characteristics. For example, the modulus of elasticity is lowest for ionically bonded compounds, while the thermal expansion coefficient increases from covalent to metallic to ionic compounds. The mechanical properties of a thin coating are different from those of the bulk.

The microstructure of CVD coatings depends mainly on deposition temperature and to a lesser extent on reactant concentration. Low temperatures result in amorphous or fine-grained coatings while at high temperatures diffusion affects strongly the microstructure.

The coating surface is usually only considered for optical reasons and not for structural reasons. However, studies of surface morphology help to understand nucleation and growth processes.

Gevelber *et al*. [Gevelber, 1996] reported the difficulty in developing the optimal deposition parameters to achieve the requirements for a selected material. The CVD method results in coatings with uniform thicknesses. Therefore, to research a new coating system, the process dynamics and interactions have to be investigated and understood. Gevelber *et al.* [Gevelber, 1996] developed a measurement-based feedback system to control the required structure.

Another thin-film deposition process is Physical Vapor Deposition (PVD). The main differences between CVD and PVD are their working parameters, such as pressure and temperature, as can be seen in Table 2.2.

Table 2.2: Comparison of CVD and PVD thin film deposition processes

CVD	PVD
pressure: 0.1 – 100 kPa	pressure: < 1 Pa (high vacuum)
Temp.: 400 – 1100 °C	Temp.: 550 °C
Formation of layers by chemical reactions of gaseous substances	Evaporation or sputtering of solid starting materials; layers formed by condensation

There are many uses and applications of the CVD thin coating technology, in chemistry, physics, biology and medicine. The applied fields range from microelectronics, solar cells, and sensors to metal cutting, corrosion protection or compatibility in medicine. Therefore, much study and research have been done to improve and advance that technology. Godse *et al.* [Godse, 1996] reported, for example, of composite CVD and PVD coatings to combine the advantages of both processes. Those coatings possess a better combination of wear resistance and chipping resistance than one of the coating processes alone.

Quinto *et al.* [Quinto, 1988] compared mechanical properties of CVD and PVD carbides coated with a layer of TiN. It was found, that the transverse rupture strength (TRS) of the ground substrates decreased after CVD coating or high temperature treatment but stayed unchanged after PVD coating. The compressive residual stresses which developed in the PVD TiN coating and the compressive stress in the WC phase increased the TRS of the PVD coated tool, as well as increased its resistance to edge chipping. The TiN coating applied by CVD is in a tensile residual stress state and its effect was lowering the TRS and its resistance to edge chipping. However, CVD coatings increased tool life in turning. The metal-cutting performance, on the other hand is better with PVD coatings, due to the greater resistance to abrasive wear and higher surface fracture strength.

Thin low pressure CVD diamond coatings are developed to produce improved cutting tools or sensors [Carlsson, 1993] [Hintermann, 1996].

2.4 CVD Coating Materials

At cutting speeds higher than 250 m/min, cutting tool inserts which are usually coated by CVD with TiC, TiN and TiCN layers are additionally coated with an Al_2O_3 layer to prolong their tool life [Berg, 1987], [Larsson, 2000]. The inner coating layer is usually a combination of TiC-TiCN-TiN to ensure good flank wear resistance (= abrasive wear) and good adhesion. The most common intermediate layer used is TiCN, and above the intermediate layer a layer of Al_2O_3, which reduces crater wear on the rake face and also acts as a thermal barrier. At the outer surface of the cutting tool insert is usually a TiN layer for aesthetical reasons because of its gold color but also to detect wear easily [Ruppi, 2001a].

The main coating layers (TiC, TiN, TiCN, Al_2O_3) which were present in the cutting tool inserts in this research project are described in detail in the following sections 2.4.1 to 2.4.4.

2.4.1 Titanium Carbide (TiC)

TiC is used as a coating layer for turning tool inserts on WC-Co substrates. However, it is also reported [Komak, 1984] that cemented TiC are used as bulk material, although they are less tough than WC-Co and have low impact resistance and low resistance to chipping.

TiC cemented carbides, however, show equal fracture toughness as WC-Co steel cutting grades and have been developed in recent years with improved properties [Doi, 1984b] [Matsubaru, 1992].

In the gas mixing unit, a mixture of titanium tetra-chloride, $TiCl_4$, methane (CH_4) and hydrogen (H_2) is produced and heated in the reaction chamber (~ 950 – 1050 °C at low pressures ~ 90 mbar). The following chemical reaction forms TiC which is deposited as [König-a]:

$TiCl_4$ (g) + CH_4 (g) $\Leftrightarrow$ 4 HCl (g) + TiC (s) (in the presence of H_2 (g))

where: (g) = gas
(s) = solid

TiC has a NaCl crystal structure. TiC has a wide homogeneity range from $TiC_{0.47}$ to $TiC_{0.96}$.

The coating of TiC is usually applied first on the WC-Co substrate. Therefore, the TiC/substrate interface is important for the adhesion of the whole coating system. The TiC coating is not only hard, inert and stable but must have good adhesion to the substrate, which depends on the microstructure and composition in the interface region substrate/coating.

This interface was studied by Skogsmo *et al.* [Skogsmo, 1984]. Cemented carbide samples in the form of very sharp needles were coated at different short coating times (30 s, 3 min, 10 min) with a thin TiC layer and the interface was investigated. The grain size of these TiC coatings was very fine (5 – 50 nm). The thinnest TiC layer was a single layer of TiC grains on the substrate. The TiC grains which were in contact with the substrate had grown in a specific orientation.

After sintering the WC-Co substrate is usually without eta-carbides or C porosity. However, during CVD of TiC, the cemented carbide substrate is easily decarburized. At the beginning of the coating process, the C for the TiC is mainly taken by the cemented carbide substrate, which results in the decarburization of the interface of the substrate and brittle eta-carbides are formed. The C is probably transported from the substrate to the coating by the Co from the binder phase, as Co is present at the substrate/coating interface. Volume shrinkage and diffusion processes lead by the eta-carbide formation can create interfacial porosity in the substrate. Skogsmo *et al.* [Skogsmo, 1984] investigated substrates which were

coated with TiC and found that they consisted of WC and the eta-phase Co_6W_6C (deposition at temperature less that 1100 °C) and probably Co_3W_3C. Using EDS, the substrate showed besides Ti, W and C, also Fe and Cr. Further, the Co content near the substrate surface had increased after deposition.

Using the Auger technique, Skogsmo *et al.* [Skogsmo, 1984] analyzed the outer atomic layers of the TiC specimen. That layer of the coating revealed a large amount of O and less C compared to the layers deeper within the coating. This suggested that the outer layers were oxidized, although that layer was only a few atomic layers thick.

Sarin [Sarin, 1983] investigated the relationship between structure and properties of CVD-TiC coatings. The influence of different hydrocarbon (CH_4 and C_3H_8) during the CVD process was investigated. The examination of the TiC structure showed two distinct grain morphologies (called zone 1 and zone 2 by Sarin [Sarin, 1983]) with a sharp transition between them. With both hydrocarbons the grain size and morphology of zone 1 and its width was identical (between 1.5 to 2 μm). The second zone 2 contained relatively uniform equiaxed grains with CH_4 and with C_3H_8 they had large non-uniform columnar TiC grains. Eta-phase was observed at the interface substrate/coating with both hydrocarbons. These observations lead to the conclusion that the first nucleation of TiC on the substrate takes place on the binder phase which is Co with W and C in solution. After nucleation, in zone 1 the growth rate is controlled by the C diffusion from the substrate, no matter which hydrocarbon is used. When the diffusion of C is delayed by the growing TiC layer and less C is available from the substrate, the controlling factor is the C in the reactor, either as CH_4 or C_3H_8, and zone 2 starts to form, which was eventually about 1.5 to 2 μm thick.

Additionally in zone 1, diffusion of the W to the TiC layer took place along the TiC submicron grain boundaries. EDS analysis and microprobe confirmed both diffusion of C and W from the WC-Co substrate to the TiC layer and also vice versa, small amounts of Ti from the coating were found in the substrate.

Sarin [Sarin, 1983] found cracks in the coating due to the high tensile stresses which were developed during the cooling cycle after coating deposition at 1000 °C. These cracks contributed to inaccurate surface hardness results. Machining tests showed the equiaxed CH_4 coating superior performance at low cutting temperatures while the columnar C_3H_8 was better at higher temperatures.

Leonhardt *et al*. [Leonhardt, 1996] also studied the influence of using different hydrocarbons at the CVD TiC deposition. When using unsaturated hydrocarbons such as CH_4, C_6H_6, etc., the CVD process was kinetically controlled and the layers had a <111> texture and showed high dislocation density. On the other hand, when using saturated hydrocarbons such as n-heptane, cycloheptane, etc, the CVD process was thermodynamically controlled, the layers had a <200> texture and had barely dislocations. The reason for the different textures can be attributed to the different stability of the hydrocarbons.

Albir [Albir, 1987] investigated eta-phases during TiC coating on WC-Co substrates. The main phases were $M_6C = Co_3W_3C$ and $M_{12}C = Co_6W_6C$. It was found, that eta-phase nucleated at 1400 °C. With the upper C concentrations M_6C was created and in the lower C concentration $M_{12}C$, which is more stable at low temperatures (< 1100 °C). Looking at fracture surfaces, a porous eta-phase was found. The porosity affected the adhesion strength of the TiC layer to the substrate. The properties of the two eta-phases can be seen in Table 2.3 [Albir, 1987].

Table 2.3: Some properties of $M_{12}C$, M_6C, WC and TiC [Albir, 1987]

	Co_6W_6C $M_{12}C$	**Co_3W_3C M_6C**	**WC**	**TiC**
at.% C	14.4 %	7.7 %	50 %	50 %
Porosity level	Low	High	--	--
Crystallographic structure	Hexagonal	Cubic	Hexagonal	Cubic
Theoretical density [g/cc]	16.064	14.576	15.7 [Exner, 1979]	4.94 [Exner, 1979]

When doing milling tests, the eta-phase caused failure.

Modifications of TiC-CVD depositions are vast. Doi *et al.* [Doi, 1984a], for example, studied TiC coatings deposited by means of modified plasma CVD and Teyssandier *et al.* [Teyssandier, 1987] did investigations on non-stoichiometric TiC deposits at high temperatures on Mo. Those non stoichiometries - up to $Ti_{0.6}C_{0.4}$ - were achieved at 1900 K under atmospheric pressure. The C/Ti ratio was highly dependent on input molar fractions of $TiCl_4$ and CH_4.

2.4.2 Titanium Nitride (TiN)

The nitrides of the group (IVA) metals, such as Ti, Zr, Hf, show high hardness and wear resistance, high melting point and high thermal and electrical conductivity. Therefore, they are used in cutting tools and wear-resistant components. TiN, for example is used as coating on conventional hardmetals to increase cutting performance [Lengauer, 1988].

During the CVD process, TiN is usually formed according to the reaction:

$$TiCl_4\ (g) + \tfrac{1}{2} N_2\ (g) + 2\ H_2\ (g) \Rightarrow TiN\ (s) + 4\ HCl\ (g)$$

(in the presence of H_2 (g))

where: (g) = gas
(s) = solid

The reaction takes place at about 800 to 900 °C and at about atmospheric pressure (900 mbar). TiN is usually used as an intermediate layer between the WC-Co substrate and the TiCN coating. The contribution of the C of the substrate to the growth of TiN is avoided by using high deposition pressures.

Further, TiN is often used as a very thin surface layer finishing a multilayer coating. If the TiN coating layer is thicker, it is used to increase wear resistance. TiN typically consists of columnar grains.

TiN is a hard material with high melting point and high density. It is also often used as additive for reinforcement of composite material. It is economical and is much studied. Shaviv [Shaviv, 1996] reported the optimum reaction parameters of TiN, such as reaction temperature, residence time, morphology of the starting material, level of impurity in rare material and preparation of the raw material mixes.

The effect of additions of TiN on the microstructure and properties of WC-based cemented carbides have been reported by Igarashi *et al.* [Igarashi, 1984]. It was found that addition of TiN increased the strength and oxidation resistance. In steel cutting, it improved chipping and thermal crack resistance but reduced crater wear resistance.

Smith *et al.* [Smith, 1987] used TiN coated steel samples and investigated flank wear during cutting operation. The coatings were between 4.5 and 5.7 μm thick. It was found that the TiN coating brought a reduction of end-point flank wear at the

cutting speed of 37.5 m/min. The rate of steady-state flank wear had been reduced by a factor between 15 and 60 times. The build-up edge area had improved, i.e. had decreased.

The effect on adhesion of TiN coatings to cemented carbides was reported by Laugier [Laugier, 1988]. Scratch tests were used to investigate coating failure at temperatures of cutting tool applications (~ 1050 °C). WC-Co substrates were coated with TiN using CVD at 1000 °C with a thickness of 6 μm. The Vickers micro hardness was 1900 HV at a load of 0.1 kgf at room temperature. Laugier found that at temperatures of about 1000 °C, the adhesion is better compared to room temperatures due to significant substrate softening.

Mechanical properties and cutting performance of TiN and TiCN coated cermets with PA-(plasma assisted) CVD at 500 to 700 °C were investigated by Richter *et al.* [Richter, 1996]. Here, the formation of brittle intermetallic phases was avoided, which was said to be a problem by other authors. It was found that with increasing substrate temperature, adhesive strength increased but hardness, wear resistance and transverse rupture strength decreased. Cutting tests showed better performance with PA-CVD coatings.

2.4.3 Titanium Carbo-Nitride (TiCN)

Titanium carbide (TiC) and titanium nitride (TiN) are isomorphous which gives a continuous series of TiC/TiN solid solutions. Both materials can exist below their stoichiometric values for C and N contents [Moskowitz, 1984]. Hardmetals, based on TiCN are called “cermets”. Those cermets consist of CN grains which have a core/rim structure surrounded by a binder (usually Co or Ni). The cores are undissolved raw material on which the rims have grown epitaxially during the sintering process [Lindahl, 1992] [Gee, 1992].

Larsen-Basse [Larsen-Basse, 1988] reported tests of some TiCN based cermets to investigate abrasive wear in cutting tool application. It was found that the

microhardness of the CN increased with increasing C content. If the cermets were bonded with different additives (Ni-Mo_2C-VC) an increase in resistance to plastic deformation (hardness) was observed as the N content increased. Tool life of these cermets was also increased, as thermal deformation resistance and thermal conductivity increased with increasing TiN content. Cutting tests were also done by Pastor [Pastor, 1988] who reported excellent performance for cutting of steel.

TiCN as a CVD coating layer is usually an intermediate layer. There are two types of TiCN deposition processes, which are distinguished by the different temperatures they take place. So called HT (= High Temperature)-TiCN coatings are deposited from $TiCl_4$-CH_3-N_2 at a temperature of 1000 °C while the so-called MT (= Moderate Temperature)-TiCN takes place at about 700 - 900 °C. The latter process is today more popular [Ruppi, 2001a]. The lower temperature reduces decarburization of the cemented carbide substrate during the coating process and reduces the brittle eta-carbides, which improves the properties of a cutting tool.

The overall reaction of the MT-TiCN reaction is the following:

$$2\ TiCl_4\ (g)\ +\ CH_3CN\ (g)\ +\ 4.5\ H_2\ (g)\ \Rightarrow\ TiCN\ (s)\ +\ CH_4\ (g)\ +\ 8\ HCl\ (g)$$

where: (g) = gaseous
(s) = solid

Deposition reactions take place at about 600 °C and continue as heterogeneous surface reactions up to 900 °C. Growth rates of the MT-TiCN coatings are typically three to five times faster than those of HT-TiCN coatings. At this high reactivity, the growth rate is not influenced by the substrate as diffusion of C through the coating is negligible. At temperature up to ~ 750 °C the deposition is mainly controlled by surface kinetics. Above 750 °C, it is mass transport controlled [Ruppi, 2001a].

The MT-TiCN coatings show columnar grain structure. SEM investigations of MT-TiCN coatings on cemented carbides of a thickness > 5 μm showed two zones of the columnar structure. Near the surface was a thin (< 1 μm) layer with randomly arranged fine granular crystals on top of which needle shaped crystals of approximately 0.1 μm diameter grow. Those needles appeared over the entire coating thickness.

The adhesive strength of MT-TiCN coatings is governed by diffusion. If the deposition temperature is increased, the bond strength improves. Therefore, materials with low diffusion such as ceramics need a higher coating temperature for good adhesion.

Residual stress in MT-TiCN coatings on cemented carbides is compressive and much lower than the stress on HT-TiCN. High wear resistance is observed with MT-TiCN coatings and they are known to possess high chemical stability and inertness against acids, alkalines and solvents, i.e. have a good corrosion resistance.
In cutting application, excellent performances are reported as flank wear is significantly reduced.

Larsson *et al.* [Larsson, 2002] reported differences of HT-TiCN and MT-TiCN coated cemented carbides. The surface morphology of HT-TiCN showed small equiaxed crystal which resulted in a smooth surface. The MT-TiCN surface had large faceted grains which were not equiaxed but had an average long axis of about 1 μm and a short axis of 250 nm. This resulted in a rough surface.

Mechanical tests showed that MT-TiCN coated tools had a higher TRS compared to HT-TiCN coated ones due to no eta-phases in the surface region and lower residual tensile stresses in the coating. MT-TiCN coated tools also showed better edge strength than HT-TiCN, due to the absence of the reversible eta-phase reaction resulting in a large number of preserved TiCN / WC interfaces.

The properties of TiCN are widely investigated to improve the coatings. Ruppi *et al.* [Ruppi, 2003] investigated MT-TiCN coatings by modifying them by carbon monoxide (CO). This resulted in grain refinement of MT-TiCN and a higher hardness from 26.4 to 32.0 GPa. With increasing CO doping, the surface smoothness was improved and friction was reduced. However, cutting tests showed a lower crater resistance.

2.4.4 Alumina (Al_2O_3)

Al_2O_3 is mostly deposited above the intermediate layers of TiC, TiN or TiCN [Chatfield, 1989] in the CVD process to reduce crater wear on the rake face and also to act as a thermal barrier.

The coating is usually deposited by hydrolysis of alumina trichloride ($AlCl_3$) at about 1050 to 1100 °C according to the overall reaction:

$$2\ AlCl_3\ (g) + 3\ CO_2\ (g) + 3\ H_2\ (g) \Rightarrow Al_2O_3\ (s) + 3\ CO\ (g) + 6\ HCl\ (g)$$

where: (g) = gas
(s) = solid

The reaction involves homogenous gas-phase reactions and heterogeneous surface reactions [Ruppi, 2001a].

Al_2O_3 exists in many forms, the most frequently used in CVD coatings is the stable α-Al_2O_3 and the two metastable κ-Al_2O_3 and γ-Al_2O_3. The properties of those three compounds are displayed in Table 2.4.

Table 2.4: Properties of stable and metastable CVD Al_2O_3

	α-Al_2O_3	**κ-Al_2O_3**	**γ-Al_2O_3**
Crystal system	trigonal	orthorhombic	cubic
Space group	R3c	$Pna2_1$	Fd3m
Lattice parameters [Å]	a = 4.7587 c = 12.9929	a = 4.8351 b = 8.3109 c = 8.9363	a = 7.92
Al atoms in unit cell	12	16	63/3
O atoms in unit cell	18	24	32
Al-co-ordination	octahedral	75 % octahedral 25 % tetrahedral	?
Density [g/cm^3]	3.99	3.77	3.64

The stable Al_2O_3 phase is α-Al_2O_3. Its crystal structure is trigonal with ABAB stacking of almost closed-packed O ions along the c-axis. Six layers of O atoms and Al atoms are in the unit cell [Vuorinen, 1990]. The CVD α-Al_2O_3 contains relatively large equiaxed grains of several micrometers (1 – 3 μm) with a high dislocation density. Voids could be found inside the α-Al_2O_3 grains and mostly at the grain boundaries.

Lux *et al.* [Lux, 1984] investigated α-Al_2O_3 coatings and reported that nucleation of α-Al_2O_3 started on single spots at the substrate surface, depending on time and temperature. It was found that impurities such as Cr, Ni, Fe, Co or Ti considerably influence growth rate and crystal morphology. Impurities can produce crystal defects, needlelike formation, whisker growth and dendritically branched structures, which are undesirable.

One of the metastable phases of Al_2O_3 is κ-Al_2O_3. It was used since the 1980s on multicoatings and many investigations were done to determine its crystal structure, e.g. [Halvarsson, 1999], [Yourdshahyan, 1999], [Gross, 1997], [Ollivier,

1997] or [Liu, 1991]. The structure is a primitive orthorhombic crystal structure with an ABAC stacking of almost close-packed O ion planes. The unit cell has four layers of O atoms with Al atoms in the interstitial positions. The Al ions are in the tetrahedral and octahedral positions in the ratio 1:3. CVD κ-Al_2O_3 coatings are composed of columnar grains, have typically a smaller grain size and have even a higher hardness and lower thermal conductivity than α-Al_2O_3.

During high speed metal cutting when high temperatures (> 1000 °C) are reached the metastable κ-Al_2O_3 can however transform to the stable α-Al_2O_3.

Halvarsson *et al.* ([Halvarsson, 1994], [Halvarsson, 1996]) report investigations of different multilayer coatings of CVD κ-Al_2O_3, and α-Al_2O_3 was present in the layers. Investigations of multilayers such as TiN/κ-Al_2O_3 coatings were done by Halvarsson *et al.* [Halvarsson, 2001] ,[Halvarsson, 1995].

Ruppi *et al.* [Ruppi, 2001b] investigated deposition characteristics as a function of temperature, pressure and H_2S concentration, since it was found that the growth rate of κ-Al_2O_3 was increased by applying H_2S doping, at 800 °C and at increasing total pressure.

As already mentioned, κ-Al_2O_3 is metastable, and it may transform to α-Al_2O_3 at high speed metal cutting [Hansson, 1995]. The rate of transformation is highly temperature dependent and Lindulf *et al.* [Lindulf, 1994] found that at 1090 °C it is three to four times faster than at 1030 °C. Nucleation of α-Al_2O_3 takes place along the transgranular cooling cracks and also not in contact with cracks.

Vuorinen *et al.* [Vuorinen, 1992] found that the $\kappa \rightarrow \alpha$-$Al_2O_3$ transformation did not change the surface morphology of the Al_2O_3 layer. CVD deposited κ- and α-Al_2O_3 showed very different morphologies. It was found that the $\kappa \rightarrow \alpha$-$Al_2O_3$ takes place by a “nucleation and growth” process. Nucleation of α-Al_2O_3 is difficult; it nucleates in as-deposited coatings at thermal cracks which are present

in the κ-Al_2O_3 layer after cooling. An 8 % volume contraction causes cracking and the adhesion of the Al_2O_3 layer to the underlying coating layer is decreased. Cutting tests were done and showed that the transformed κ-Al_2O_3 flaked severely at the beginning of cutting. That led to reduced diffusion wear resistance and crater wear.
Ruppi *et al.* [Ruppi, 1999] confirmed that phase transformation during metal cutting took place. It occurred locally in the κ-Al_2O_3 coating on the rake face. The examinations showed that the κ→α-Al_2O_3 transformation occurred in many turning operations and crater wear of κ-Al_2O_3 occurs under such conditions via plastic deformation and ductile fracture of the α-Al_2O_3 phase formed as a result of the phase transformation.

The metastable γ-Al_2O_3 phase exhibits a face centre cubic ABC stacking of O. Its structure is a "defect cubic spinel structure" with vacancies in part of the cation positions. Larsson *et al.* [Larsson, 2001] reported microstructure and properties of CVD γ-Al_2O_3 coatings. They were fine-grained with high density of {111} growth twins and contained some residual S (~ 0.8 %). It grew epitaxially on the substrate. The texture of the substrates was reflected in the γ-Al_2O_3.

Mechanical properties of the Al_2O_3 phases have been investigated. Sönderlund *et al.* [Sönderlund, 1994] studied hardness and elastic modulus of κ- and α-Al_2O_3 coatings. It showed that κ-Al_2O_3 had strong anisotropy in hardness and elastic modulus. They are both significantly higher in the direction parallel to the growth direction than in the perpendicular direction. κ-Al_2O_3 showed a strong microstructural anisotropy with columnar grains oriented in the growth direction. α-Al_2O_3 did not show any anisotropy in the microstructure. Jämting *et al.* [Jämting, 1995] found that κ-Al_2O_3 was harder than α-Al_2O_3 and also showed a higher elastic modulus.

Osada *et al.* [Osada, 2005] reported wear mechanisms of transformed α-Al_2O_3 by different heat-treatment processes. The α-Al_2O_3 which was continuously

transformed without cooling, after deposited as κ-Al_2O_3 showed high wear resistance, because the microcracks that were generated during the heat-treatment before cooling were uniformly dispersed in the layer and cooling cracks with wide width did not exist.

2.5 Hardness

Hardness is the resistance of a solid to local deformation [Tabor, 1970]. Hard materials show high cohesive energy, short bond length and a high degree of covalent bonding. Hardness measurement involves usually large localized stresses beneath an indenter. The deformation mechanism depends on temperature, crystal orientation, indenter shape and the size of the indenter.

Indentation damage in WC and (W,Ti)C, which are usually the main constituents of metal machining tools were investigated between room temperature and 1000 °C with loads up to 450 N [Rowcliffe, 1983]. Plastic flow occurred in the WC crystals to adjust the stress and cracks formed between room temperature and 400 °C. Above 400 °C, crack-free impressions were produced. In (W,Ti)C, radial cracks occurred down to at least 1 N. Above 10 N, lateral cracks emerged at the surface, interacted with radial cracks and caused surface spalling.

The hardness of thin coatings can also vary due to changes in film texture, as films deposited by PVD or CVD processes usually show a strong preferred orientation. Closed packed planes usually grow parallel to the substrate surface. This texture is strongly dependent on the growth parameters.

The actual measurement of the hardness of coatings is difficult and formulae to express it are widely searched ([Burnett, 1987a], [Burnett, 1987b]).

One model is given by

$$H_c = H_s + \alpha (H_f - H_s)$$

where: `
H_c = composite hardness
H_s = substrate hardness
H_f = film hardness
α = empirical derived, material-independent factor

The formula relates the film hardness to the individual hardnesses of the substrate and the composite.

Jönsson *et al.* [Jönsson, 1984] used a geometrical approach to divide the contributions of substrate and coating.

The hardness of the film H_f is given by

$$H_f = H_s + \frac{H_c - H_s}{2 C_{1,2} \frac{t}{D} - C_{1,2}^2 \left(\frac{t}{D}\right)^2}$$

where: $C_{1,2}$ = geometrical constant, which stands for C_1 or C_2, depending on substrate/coating combination
$C_1 = \sin^2 (11°)$ for hard coating and soft substrates
$C_2 = 2 \sin^2 (22°)$ for similar hardness of coating and substrate
t = film thickness
D = indentation depth

In the case of the present project $C_1 = C_2$.

2.6 Wear Resistance

Nowadays, the life of a tool cutting edge is counted in minutes and tool lives have an established average mark of about fifteen minutes. A modern cemented carbide cutting tool edge penetrates a large amount of metal during its life. For instance, at a cutting speed (V_c) of 200 m/min and with a cutting depth (a_p) of 3 mm, the material area that passes the edge every second is 10,000 mm^2. This is more than 0.5 m^2 of material past the edge every minute. During a tool-life of 15 minutes, the small 3 mm length of cutting edge will have had 9 m^2 of material passing the face and flank under the extreme conditions of machining, see Fig. 2.13 as an illustration [AB Sandvik, 1994].

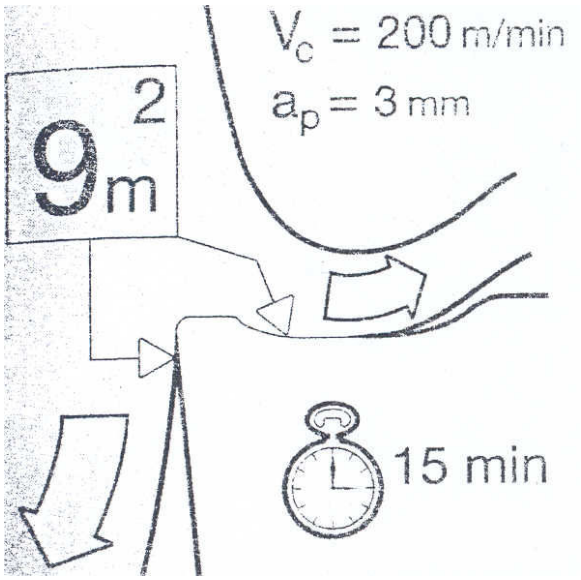

Fig. 2.13: Amount of metal passing the edge [AB Sandvik, 1994]

Wear is the result of interaction between tool, workpiece material and machining conditions. The life of the cutting edges is affected by several loads, which strive to change the geometry of the edge. The main ones are mechanical, thermal, chemical and abrasive loads.

As a result of loads exerted on the cutting edge during machining, many wear mechanisms dominate metal cutting [Östberg, 2005], such as abrasive wear (1),

diffusion wear (2), oxidation wear (3), fatigue wear (static or dynamic) (4) and adhesion wear (5), see the illustration in Fig. 2.14 [AB Sandvik, 1994].

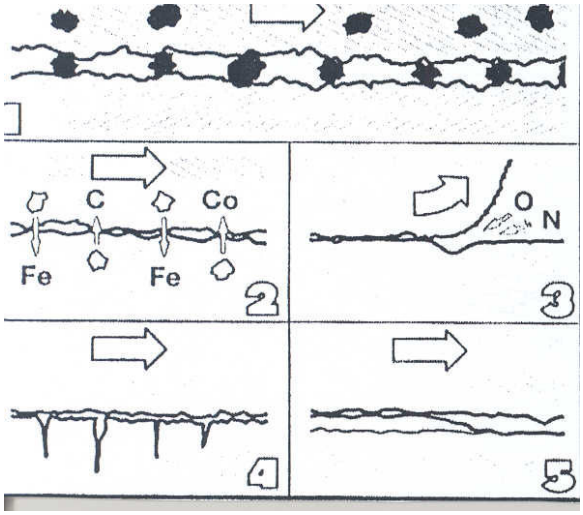

Fig 2.14: Basic wear mechanisms in metal cutting [AB Sandvik, 1994]

Abrasive wear is very common and is caused mainly by the hard particles of the workpiece material. It is a result of the mechanical load on the insert that leads to the wearing of a flat face on the cutting edge flank. To resist abrasive wear, the hardness of the cutting tool is of uppermost importance.
Diffusion wear is affected by chemical factors during the cutting process. The chemical properties of the tool material and the affinity of the tool material to the workpiece material will affect the diffusion wear mechanisms. Some cutting tool materials are inert against most workpiece material, while some have high affinity to some. WC and steel have affinity towards each other leading to diffusion wear. This results in the formation of a crater on the chip face of the inserts. Diffusion wear is temperature dependent and greatest at high cutting speeds.
High temperature and the presence of air mean oxidation for most metals. W and Co form porous oxide films which are more easily rubbed off by the chip.
Fatigue wear is often thermo-mechanical. Temperature fluctuations and the application and removal of cutting forces can lead to cutting edges cracking and breaking. It can also occur from the cutting forces being too high for the mechanical strength of the cutting edges.

Adhesion wear occurs mainly at low machining temperatures on the chip face of the tool. That often leads to the formation of a built-up edge, between the chip and the edge.

The main regions of tool wear on a cutting edge are the chip face (A), the flank of the leading clearance face (B) and the flank of the trailing clearance face (C) as well as the actual nose or parallel land area (D) (see Fig. 2.15 [AB Sandvik, 1994]).

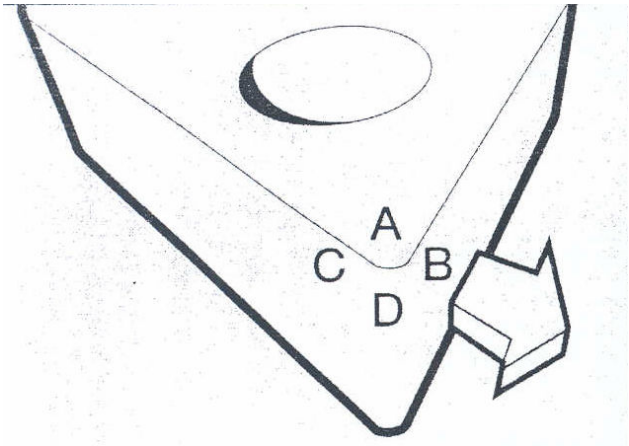

Fig. 2.15: Places of wear on insert [AB Sandvik, 1994]

The classification of tool wear types are shown in Fig. 2.16 [AB Sandvik, 1994].